DARHT ACCELERATORS UPDATE AND PLANS FOR INITIAL OPERATION*

M.J. Burns, B.E. Carlsten, T.J.T. Kwan, D.C. Moir, D.S. Prono, S.A. Watson
Los Alamos National Laboratory, P.O Box 1663, Los Alamos, NM 87544

E.L. Burgess, H.L. Rutkowski
E.O. Lawrence Berkeley National Laboratory, 1 Cyclotron Rd., Berkeley, CA 94720

G.J. Caporaso, Y.-J. Chen, Y. J. (Judy) Chen, S. Sampayan and G. Westenskow
Lawrence Livermore National Laboratory, 7000 East Ave., Livermore, CA 94550

Abstract

The Dual-Axis Radiographic Hydrodynamics Test (DARHT) facility will use two perpendicular electron Linear Induction Accelerators to produce intense, bremsstrahlung x-ray pulses for flash radiography. We intend to produce measurements containing three-dimensional information with sub-millimeter spatial resolution of the interior features of very dense explosively driven objects. The facility will be completed in two phases with the first operational by June 1999 utilizing a single-pulse, 19.8-MeV, 2 to 4-kA, 60-ns accelerator (activated in March 1999), a high-resolution electro-optical x-ray imaging system, and other hydrodynamics testing systems. The second phase will be operational by Sept. 2002 and features the addition of a 20-MeV, 2 to 4-kA, 2-microsecond accelerator. Four short electron micropulses of variable pulse-width and spacing will be chopped out of the original, long accelerator pulse for producing time-resolved x-ray images. The second phase also features an extended, high-resolution electro-optical x-ray system with a framing speed of about 2-Mhz. In this paper we will present a Figure-Of-Merit for a x-ray based flash radiography system to motivate the selection of accelerator parameters. We will then present sub-system performance measurements from Phase 1, the physics of the interaction of our high-intensity beams with the x-ray conversion target, initial Phase 1 accelerator measurements (if available), and plans for operation. We will also discuss designs and prototype testing results for the 2-microsecond Phase 2 accelerator, including prototype induction cells and pulsed power, prototype kicker magnet performance to chop the beam, and design considerations for a multipulse x-ray conversion target.

1 INTRODUCTION

Maintenance of a smaller, aging U.S. nuclear weapons stockpile without underground nuclear testing (UGT) requires the capability to verify and benchmark the complex computer calculations on which stockpile confidence will be based. A key to this capability will be evaluation of the primaries of U.S. nuclear weapons through non-nuclear hydrodynamic testing, or "hydrotesting". These tests utilize very powerful x-ray sources to radiograph a full-scale, non-nuclear mock-up of a nuclear weapon primary during the late stages of the implosion, returning data on shapes, densities, and edge locations. (In the future, other probes such as tens-of-GeV-energy proton beams may also be used.) DARHT will be the first hydrotesting facility in the post-UGT era and will address evolving DOE requirements by developing images with sub-millimeter resolution, from two views (the minimum for large-scale three-dimensional information), and with multiple views along one axis.

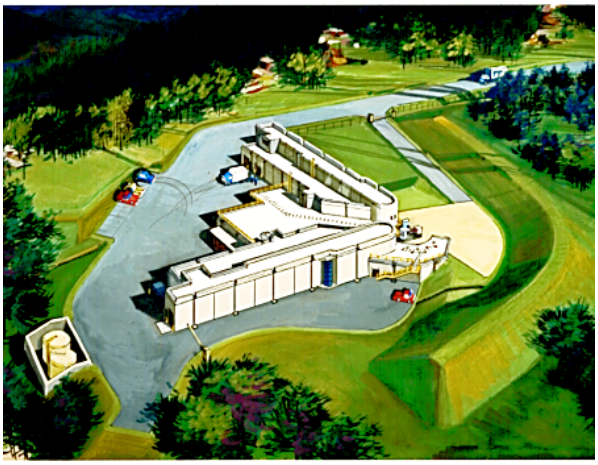

Figure 1: Artist's rendition of the DARHT facility

We will present the current status of DARHT by first describing in Section 2 a Figure-of-Merit for radiographic hydrotesting that motivates parameter selection for the DARHT accelerators. In Section 3 we will present the status of Phase 1 of DARHT. In Section 4 we will discuss Phase 2, featuring the second x-ray system with multipulsing capability. Section 5 discusses the schedules and plans for initial operations of both phases.

* Work supported by the U.S. Department of Energy under contracts W-7405-Eng-36 (LANL), DE-AC03-76SF00098 (LBNL), and W-7405-Eng-48 (LLNL)

2 RADIOGRAPHIC FOM

Each leg of DARHT is a x-ray imaging system. Two simultaneous images from perpendicular directions are the minimum required for 3D data and thus the essential layout of the facility is determined. An information theory based Figure-of-Merit (FOM), using the general radiographic system schematic shown in Fig. 2, has been developed to help describe the design of DARHT.

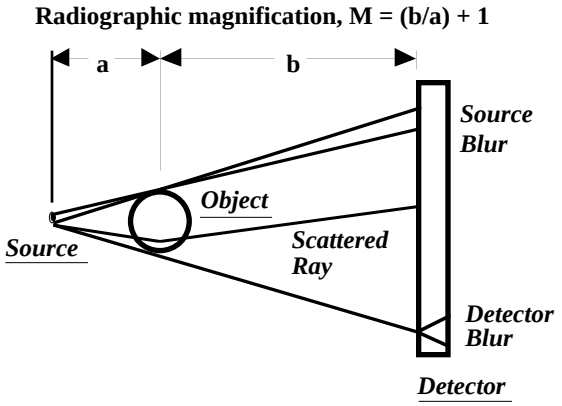

Figure 2: Radiographic system schematic

We tightly focus the electron beam from the accelerator onto a high-Z x-ray conversion target. X-rays are attenuated through the object that has been explosively compressed at velocities of many km/sec. An ~250,000 element segmented scintillator that converts x-rays to light, which is lens-coupled onto a mosaic of large-area charge-coupled devices (CCD).

A minimum description of the x-ray system must consist of parameters describing the source, object, detector, and experimental geometry. Source parameters are the spot size (S, mm, the diameter of an equivalent, uniformly illuminated disk at 50% modulation, or about 1.6 times greater than a Gaussian FWHM description [1]), the x-ray dose (D, Roentgens, R, @ 1-m distance from the source), the number, N(E), of x-ray photons per square-mm per R @ 1-m (a function of the electron beam energy, E), and the x-ray pulse width, τ, μsec. The object parameters are the average object transmission, T, and the characteristic velocity, V (km/sec. The detector parameters are the detective quantum efficiency, QE, the cut-off frequency (detector blur), F_c (cycles/mm at 50% modulation), and the scintillator pixel size in the object plane, P (mm). Finally, the first radiographic conjugate, a (m), and the radiographic magnification, M (see Fig. 2), describe the geometry.

The FOM is developed as the product of the system blur (characterized by the MTFA [2], or area under the Modulation Transfer Function curve for the system) and the amplitude signal-to-noise ratio (SNR). Our simple SNR model assumes Poisson counting statistics and is proportional to the square root of the number of recorded quanta. This model neglects noise from situation-dependent sources (such as x-ray scatter, see below). Every doubling of the amplitude SNR doubles the quantization levels and thus increases the dynamic range by one-bit. Thus, information (in bits) increases as the base-2 logarithm of the amplitude SNR.

The MTFA is inversely proportional to the three principal blurs (source blur, detector blur, and object motion blur) added in quadruture. We approximate the 50% modulation frequency of each blur, convert to an equivalent spatial blur (strictly valid only for Gaussian blurs), and assume no aliasing effects.

Our system FOM (proportional to bits/pixel) is:

$$\mathrm{FOM} = (\mathrm{MFTA})\,\mathrm{Log}_2(1 + \mathrm{SNR}) = \frac{\mathrm{Log}_2\left(1+\frac{P}{a}\sqrt{N(E)\,D\,T\,QE}\right)}{\sqrt{2\left[\frac{(M-1)S}{M}\right]^2+\left[\frac{1}{M\,F_c}\right]^2+2[V\tau]^2}}$$

This is a slowly varying quantity with a larger FOM value indicative of a higher quality x-ray system.

Although this FOM is useful for general comparisons of x-ray imaging systems, quantitative system design is also "task" dependent. For DARHT, the task is to precisely identify edges within the object. Other tasks could result in different system parameter optimization than selected for DARHT.

In the past, x-ray scatter has limited the resolution of dense-object images using MeV-radiography. Generally, x-ray scatter causes a background noise in the image and has been partially mitigated by "graded collimation" (being thick where the object is thin and thin where the object is thick. This helps to control scatter and also reduces the dynamic ranger required in the detector). Proper electron beam energy selection has been required to best match the bremsstrahlung spectrum with the objects of interest. We find an optimum electron beam energy between 12-20 MeV that balances photoelectric absorption and Thompson scattering (the predominant scatter mechanisms at low energy) with Compton scattering and pair production (more important at high energies). X-ray dose is almost a cubic power of the beam energy and therefore we pick the highest energy practicable with respect to scatter, or 20-MeV.

A short pulse-width is needed to reduce motion blur. High peak currents are then required to generate sufficient x-ray dose (dose being proportional to the total charge striking the conversion target). We selected a Linear Induction Accelerator to provide the required high dose at moderate energy with short pulse length. Consideration of the FOM shows that a preoccupation with dose is not warranted because the spot blurs and detector blurs are dominant. Therefore, the design of the DARHT accelerators is driven most by the need to generate a small spot size and with a sensitive detector design of high cut-off frequency. Table 1 lists the design parameters.

Table 1: DARHT system parameters		
Parameter	*Phase 1*	*Phase 2*
Spot size (mm)	1.2 - 2.0	1.2 - 2.0
Dose (R@1m)	500 - 1000	Max. 650-1000
Pulse width (ns)	60	variable to 80
DQE (%)	≥30	≥20
F_c (cycles/mm)	≥0.3 (-3dB)	≥0.3 (-3dB)
Pixel Size (mm)	0.9 x 0.9	1 x 1
1st conjugate (m)	0.8 to 1.5	1.1
Magnification	≤ 4	≤ 4
Accelerator Parameters		
Energy (MeV)	19.8	20.0
Current (kA)	2 - 4	2 – 4
Pulse width (ns)	60	2000
Energy spread	< ± 1%	< ± 1%
Norm. emittance (4-rms, πcm-rad)	0.15	0.15
Grad. (MeV/m)	0.47	0.35

3 PHASE 1

Phase 1 accelerator components (Fig. 3) have been tested on the Integrated Test Stand, or ITS [3], consisting of the injector and 8 induction cells. Other principal components for the full system include 56 additional cells, the single-pulse detector and high-explosive containment structures.

Figure 3: Phase 1 injector and accelerator

The 60-ft. long Phase 1 injector [4] consists of a prime power supply (a 3.0-μF/120-kV capacitor bank switched through the primary of a 1:15 Stangenes iron-core autotransformer by an air-blown spark gap) that pulse-charges a glycol Blumlein. The 6-ft. diam. Blumlein (7.65-Ω inner line, 7.3-Ω outer line, pulse-charged to 1.5-MV in 4.6-μs) discharges via 4 laser-triggered spark gaps (0.7-ns 1-σ jitter) into a series of three transmission lines with impedance changes to step-up the voltage to 4-MV at the diode. The vacuum diode consists of a 170-Ω liquid resistor load in parallel with the 181-mm A-K gap and has a 10-90% risetime of 20-ns. A flat, 64-mm diameter velvet emitter is used to produce 2-kA at 3.75-MeV. A 90-mm cathode is used to generate 4-kA.

The accelerator consists of 64, 0.25-MV induction cells [5]. Each has a 148.2-mm-diam. bore, a 19.1-mm accelerating gap, 11 oil-insulated TDK PE16B nickel-iron-zinc ferrite toroids (237-mm ID, 503-mm OD, 25.4-mm thick), a cross-linked polystyrene insulator (ε=2.5), a quadrufilar-wound solenoid magnet with homogenizer rings [6], two cosine-wound dipole trim magnets, and a cosine-wound quadrupole magnet (to compensate for the weak quadrupole field introduced on-axis by the pulse-power feed to the cells). 818 individual ferrite toroids were measured and sorted into individual cell groupings resulting in each cell having 27.93-mV-s with σ=0.61%. 66 solenoids (64 plus spares) were measured to have an average maximum tilt (defined at the largest transverse magnetic field on axis divided by the axial field at that point) of 0.35-mrad (σ=0.17-mrad) and 0.90-mrad (σ=0.48-mrad) after installation in the cells. Beam Break-Up parameters have been measured with both the TSD method and by measuring transverse oscillations on the ITS beam [7]. At the principal resonant frequency of 790-MHz, the real (reZ) and imaginary (imZ) parts of the transverse impedance in the horizontal (X) and vertical (Y) planes are reZ_X=6.03Ω/cm±5%, reZ_Y= 6.45Ω/cm±5%, imZ_X=-1.0Ω/cm±1.0Ω/cm, imZ_Y= 5.5Ω/cm±1.0Ω/cm. The quality factors are Q_X=4.6 and Q_Y=5.5.

Thirty-two water-insulated, 11-Ω, 0.25-MV Blumleins with coaxial midplane-triggered switches operating in SF_6 drive two cells each through four DS 2158 44-Ω cables. Each Blumlein charging unit has two 1.4-μF/40-kV capacitors switched via two parallel EEV CS-1722 thyratrons into a 1:11 step-up transformer to pulse-charge the line in 5-μs. An independent trigger is supplied for each Blumlein consisting of two 30-nF/70-kV capacitors switched by a EEV CX-1725 thyratron into a 1:4 step-up transformer to drive a magnetic pulse-compressor to supply a 200-kV/10-ns risetime pulse to the trigger cable. Typical system jitter is <1-ns (1σ) for any consecutive 100 shots. The Blumleins provide a 67-ns pulse to the cells with a 0.6%-rms variation over the beam pulse-width of 60-ns.

Beam is transported to the x-ray conversion target via simple solenoid transport. Maintenance of a 1.2-2.0-mm electron beam spot with a front surface power density of 0.3-1.7 TW/cm^2 is one of the principal design challenges. At these energy density levels the target material or surface contaminants may be ionized and the ions accelerated into the beam due to space charge forces. This can partially charge neutralize the beam, causing a pinch upstream of the target and subsequent overforcusing at the

target [8] leading to x-ray spot size growth as the pinch point moves upstream. Experiments at the ITS (Fig. 4) showed a growth in the radiographic spot size at 3.3-mm, 5.5-MeV, 2.8-kA, and 60-ns. Other experiments [9] at 5-MeV, 2-kA, 40-ns, and 2-3-mm focus have not observed the effect. When the phenomena is present, resistively isolating the target from ground has been found to be effective (see Fig. 4 and Ref. [8]). The intercepted charge "self-biases" the target, overcoming the beam self-field and trapping ions within about 1-cm of the target surface.

One theory explaining the ITS results [8] requires

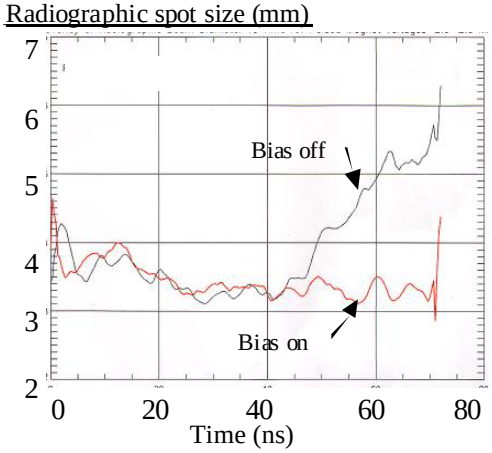

Figure 4: Time-resolved radiographic spot size measurements from the ITS

sufficient energy be deposited in the target material to cause boiling. Therefore target material with a high specific heat and high boiling point, while maintaining the high-atomic number and high density required for efficient x-ray production, may also be of use. Tantalum silicide ($TaSi_2$) and a Ta-Nb-V alloy (62.5Ta-30Nb-7.5V) are two such materials. Experiments at DARHT will begin initially at 2-kA/2-mm and focus on the use of special target material and a clean environment. As current density is increased, a barrier upstream of the target to limit ion migration and the biased-target may be used.

The phase 1 detector consists of a 55-cm-diam. x 2-cm-thick segmented BGO scintillator array with 250,000 polished 1mm x 1mm x 20mm pixels [10]. The x-ray scintillation light is lens coupled with 5, fixed conjugate, 165mm, f1.1 lenses [11] to a mosaic of 5, SITe SI424A [12], back-thinned CCD's (125cm^2 effective area). This combination results in a highly quantum efficient, linear detector (DQE > 30%) with better than 20uR sensitivity.

4 PHASE 2

Phase 2 is a collaboration between LANL, LBNL, and LLNL. It will produce the second x-ray system necessary to generate 3D data. This system will also produce four high-resolution images within a 2-μs time window. We will generate a 2-μs, 20-MeV, 2-4-kA LIA electron beam and use a fast deflection system to select four short (<80-ns) micropulses to be focused on a 4-pulse target system. The resulting x-ray images will be captured on a 4-pulse extension of the Phase 1 detector.

Space restrictions within the existing DARHT facility force the injector to occupy two levels. On the bottom level is the Marx prime power feeding a vertical insulating column that drives a flat, 16.5-cm dia. dispenser-cathode with polished stainless steel electrodes. The Marx consists of 88 type E PFN stages driving a matched load at 3.2-MV with a 400-ns rise, 2-μs flat pulse. The 444.5-cm tall, oil-filled insulator column has both alumina and Mycalex insulating rings. The peak electric field stress on the cathode shroud is 120-kV/cm with 2-kA beam current. The design beam emittance (norm,4-rms) is 0.05-πcm-rad.

There are two types of induction cells. The first eight have a 35.56-cm dia. beam pipe and run at 173-kV while the remaining 80 have a 25.40-cm dia. pipe and supply 193-kV. The larger bore cells intercept essentially no beam from the injector rise time and reduce transverse impedance in a region susceptible to BBU because of the low transport field. All of the oil insulated cells use 4 individual cores of Allied Signal 2605SC Metglas with either 0.48 V-sec core capacity or 0.43 V-sec in the large bore cells. A 200-ns rise-time leads to a 2.02-μs flattop. A Mycalex conical insulator is used in each cell is for its excellent breakdown and mechanical properties. Each individually mounted cell contains a transport solenoid and a steering coil. Ferrite damping is employed to reduce the cell quality factor.

Each induction cell has an individual cell-driver which contains 4, 7-section E-network PFNs in a Marx configuration. Each driver has a 20-Ω impedance and will deliver a 2.4-μs flattop into a resistive load of 5-Ω for a total drive current of 10-kA at 200kV. To compensate for the non-linear magnetization current of the Metglass cores, the PFN impedance varies from front to back. The impedance of each PFN can also be reduced 20% to tune for a ±0.5% flattop.

The principal element of the beam transport section is the fast deflector, or kicker system [13], used to generate four micropulses from the primary accelerator beam. It is similar in design to stripline beam position monitors. There are four equal size electrodes enclosed within a vacuum housing that has a DC bias magnetic dipole wound over the enclosure. An opposite pair of electrodes is driven by a fast amplifier through transit time isolated 50-Ω cables to provide beam deflection. The other two electrodes are terminated at their 50-Ω matched impedance. A subsequent drift space of several meters allows a substantial relative deflection to develop between the output beam positions of the kicker and drift. A DC septum magnet allows the separation of the two output beams. The bias dipole will deflect the beam off-axis into a dipole field region of the septum that will transport the beam into a dump. When an x-ray pulse is desired the kicker pulsers are activated and overcome the bias field allowing a short segment of beam to travel down the axis through a null field region of the septum and on to the x-

ray converter target.

The initial 4-pulse target will consist of a large number (of order 20) of thin (approximately .05 mm) tungsten sheets separated by vacuum gaps with an overall thickness of about 1 cm (we are also exploring the use of a low density "foamed" target). The sheets are held within a tungsten cylinder that provides radial confinement of the target. Distributing the target over an extended distance delays the axial outflow of plasma and permits the generation of four x-ray pulses over a period of 2-μs. Operating the target in good vacuum (< 10^{-7} Torr) will reduce the light contaminants on the surface to the level that the first pulse to disrupt the target focus will generate insufficient ions. Typically the first pulse will convert much of the target into a plasma. Subsequent pulses can be protected from backstreaming ions by using either a target bias or an inductive ion trap placed immediately upstream of the target. Plasma lengths over 2-μs (< 2 cm.) will not significantly disrupt the focal spot.

Prototype accelerator components will be evaluated on a long-pulse electron beam test stand assembled around the THOR [14] diode. THOR generates a 2-μs, ≤4-MeV, and ≤3.2-kA beam with an integrated beam emittance of 0.5-1.0 cm-rad, sufficient for evaluating long-pulse DARHT components. Two prototype induction cells will be tested through September 1999, to investigate effects of beam interception on the cell insulator, including breakdown and focusing/steering effects due to plasma generation. Then

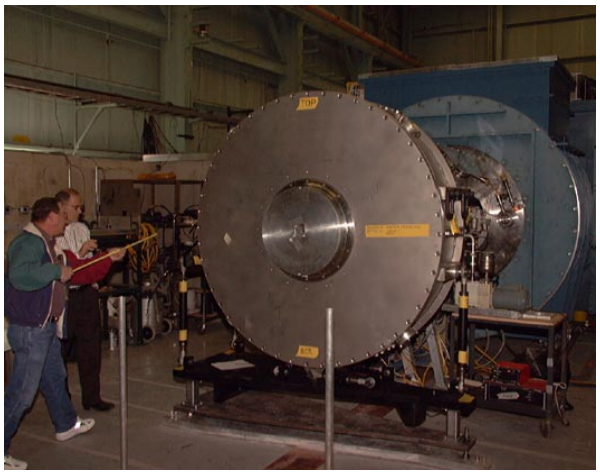

Figure 5: A Phase 2 induction cell on the THOR diode

8 induction cells, kicker, and multiple-pulse target components will be evaluated. In addition long-pulse beam current, centroid, and profile measurement diagnostics will be evaluated.

The phase 2 detector is an extension of the single pulse BGO detector. It utilizes a 40cm diam. x 3cm thick, segmented LSO scintillator array. LSO [15] was chosen because of its unique combination of high brightness, high density, and fast time constant. This array will also be lens coupled to a variety of special purpose frame shuttered CCD's under development at MIT-LL, Princeton Instruments, and SITe.

5. PLANS FOR INITIAL OPERATIONS

Phase 1 injector start-up has begun with full accelerator operation by May 1999. By June 1999 we expect a 2-mm (1.3-mm FWHM) x-ray spot and 500 R @ 1-m, sufficient to meet the project's radiographic resolution requirements. Increased beam current and advanced target designs will be introduced later with the goal of achieving a 1.2-mm spot and 1000 R @1-m.

Phase 2 prototype testing is underway. Injector installation during the second half of 2000 will be followed by phased accelerator operation for the next year. A year of full system commissioning is planned ending in Phase 2 hydrotesting operations by the end of Sept. 2002. The Initial Operating Capability will be at 2-kA using a simple target system. The beam current will be increased and more advanced target designs introduced during the operations. The installation of additional beamlines utilizing the dumped fraction of the beam for more views of the object and higher order 3D data may also be considered at that time.

6 REFERENCES

[1] Mueller, K., "Measurement and Characterization of X-Ray Spot Size", *Proceedings of the Flash Radiology Topical*, American Defense Preparedness Assoc., 1989.

[2] Holst, G.C., *Sampling, Aliasing, and Data Fidelity for Electronic Imaging Systems, Communications, and Data Acquisition*, SPIE JCD Publishing, 1998.

[3] Burns, M.J. et al, "Status of the Dual-Axis Radiographic Hydrotest Facility", *Proc. of the XVIII Intl. Linear Accel. Conf.*, Geneva, Switzerland, 1996

[4] Downing, J.N. et al, "Pulsed Power Systems for the DARHT Accelerators", *IEEE 1991 Part. Accel. Conf.*, San Francisco, CA, 1991

[5] Burns, M.J. et al, "Cell Design for the DARHT Linear Induction Accelerators", ", *IEEE 1991 Part. Accel. Conf.*, San Francisco, CA

[6] Burns, M.J. et al, "Magnet Design for the DARHT Linear Induction Accelerators", ", *IEEE 1991 Part. Accel. Conf.*, San Francisco, CA

[7] Alison, P. and Moir, D.C., "BBU Gain Measurements on the ITS 6-MeV, 4-kA Linac", *Proc. of the 1997 Part. Accel. Conf.*, Vancouver, Canada, 1997

[8] Kwan, T.J.T, "Electron Beam-Target Interaction in X-Ray Radiography", LA-UR-98-4802, submitted to *Physics of Plasmas*, 1998

[9] Sampayan, S., et al,"Experimental Investigation of Beam Optics Issues at the Bremsstrahlung Converters for Radiographic Applications", *Proc. of the 1998 Linear Accelerator Conference*

[10] Watson, S.A. et al, "Solid and Segmented Scintillator Performance in a Co60 Test Stand", *DARHT Tech. Memo. No. 93*, Los Alamos National Laboratory, 1998

[11] Watson, S.A. et al, "The DARHT Radiographic Camera Lenses: Design and Performance", *DARHT Tech. Memo. No. 98*, 1998

[12] Scientific Imaging Technologies, Inc., "SITe 2048 x 2048 Scientific-Grade CCD", 1994

[13] Chen, Y.J.(Judy), et al, "Precision Fast Kickers For Kiloampere Electron Beams", proceedings of this conference.

[14] R. F. Schneider, J. D. Miller, W. C. Freeman, M. J. Rhee, D. J. Weidman, J. Pasour, and K. T. Nguyen, "THOR, a long-pulse electron beam generator design and performance characteristics," 8th IEEE Pulsed Power Conference, San Diego, 1991

[15] Melcher, C.L. et al, "Cerium-doped Lutetium Oxyorthosilicate: A Fast, Efficient New Scintillator", *IEEE Trans. Nucl. Sci.*, **NS-39**, 1992.